

Magnetic Reconnection

School:

Los Alamos High School
1300 Diamond Dr.
Los Alamos, NM 87544

Team Members:

Tate D. Plohr

Project Mentor:

Dr. Mark Petersen

MAGNETIC RECONNECTION

Tate D. Plohr

ABSTRACT

Magnetic reconnection is the reconfiguration of magnetic field lines in plasma. It is a phenomenon that drives solar flares and Coronal Mass Ejections (CMEs) on the Sun's surface. Strong CMEs and solar flares are capable of affecting Earth by damaging electrical equipment, disrupting communication, and harming astronauts in space. In my project, I wrote a Python program that simulates the onset of magnetic reconnection. I have used my program to understand conditions that lead to magnetic reconnection. In summary, I have found that increased magnetic field strength and increased plasma resistivity stabilize a current sheet and consequently facilitate magnetic reconnection. This understanding is essential for developing predictive models of magnetic reconnection that help mitigate the catastrophic damages caused by CMEs or solar flares.

INTRODUCTION

On the surface of the Sun, many powerful phenomena occur. As fascinating as they are, they have the potential to harm people on Earth. Massive arches of plasma, called coronal arches, constantly generate solar wind that bombards the Earth's magnetic field. In addition, if they are big enough, the arches can create solar flares and Coronal Mass Ejections (CMEs), which are even more powerful. Solar flares and solar wind emit strong electromagnetic radiation, including radio waves and ultraviolet radiation, which can disrupt communication and harm astronauts in space as well as people at high altitudes in airplanes. Along with radiation, plasma from the sun's surface can be propelled towards Earth by CMEs. If the plasma hits Earth, it can cause electrical failures and cut communication lines. Such an event could be disastrous in many ways. For instance, in hospitals without secure or backup power, life-supporting devices could become dysfunctional. For the United States alone, it is estimated that a CME could cost tens of billions of dollars [1]. For example, in September 1859, a massive CME hit Earth and caused the Carrington Event. The Carrington Event was so strong that auroras, which are a result of the interaction between Earth's magnetic field and solar plasmas, were seen near the equator, compasses failed to point North, and telegraphs threw sparks and transmitted messages without a battery connected [2]. A CME on the scale of the Carrington event or larger would undoubtedly cause more serious complications in our modern world, where much more than telegraph lines are powered by electricity.

Therefore, it is very important to mitigate the damage caused by these phenomena. Doing so requires early prediction of a large solar flare or CME [3]. However, our prediction methods are currently only able to detect solar flares or CMEs right before they start coming towards us. We have little time to prepare.

The mechanism behind these dangerous phenomena that drives the massive burst of energy is magnetic reconnection [4] (See Fig. 1.). Magnetic reconnection occurs when two opposing magnetic field lines reconfigure to form a new magnetic system. This releases tremendous energy by converting magnetic potential energy into kinetic energy of the coronal plasma [5]. The accelerated plasma creates solar wind, solar flares, and CMEs. Understanding the dynamics of magnetic reconnection, particularly its onset, is vital to predicting when a solar flare or CME will form.

The standard model of magnetic reconnection is the Sweet-Parker model, also known as a current sheet or magnetic separatrix. Figure 1 is a schematic diagram of the process. Each of the three stages also represents the three main topics of magnetic reconnection; (a) whether or how two magnetic fields come close to initiate reconnection, *i.e.*, onset problem; (b) how fast reconnection happens, *i.e.* rate problem; (c) how much magnetic energy will be converted to kinetic energy, *i.e.* energy partition problem.

The standard model of Magnetic Reconnection is called the **Sweet-Parker model**, also known as a **current sheet**.

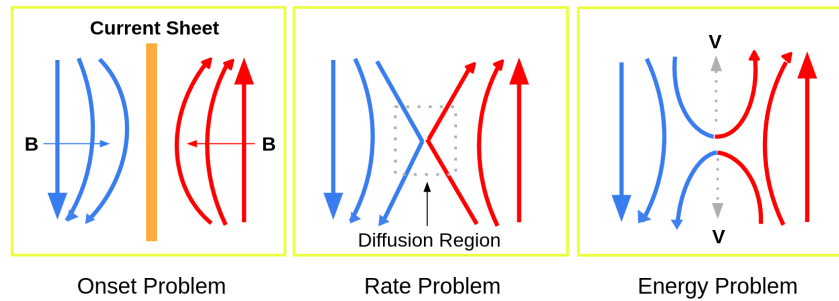


Figure 1. Schematic diagram of magnetic reconnection (a) Two magnetic fields come toward each other; (b) via diffusion they reconnect; (c) the new field lines carry away plasma (with very high energy).

In this paper, we are interested in the stability of a current sheet to see its validity as a model for the onset of magnetic reconnection. Hence our focus is on (a) in Figure 1. We assume that the flow is incompressible, i.e., the mass density is uniform, because it has been shown that compressible flow is more stable [6]. An incompressible current sheet is described by two variables: the fluid velocity and the magnetic field. In an idealized configuration, both are in the vertical direction.

The velocity field of the current sheet is called the Bickley Jet in fluid dynamics (when there is no magnetic field) and is known to be unstable. There is a name for the kind of instability that the jet is subject to: the Kelvin-Helmholtz instability. With a sinusoidal perturbation in the vorticity field, chains of vortices spread out from the jet to the left and right, as shown in the figure below.

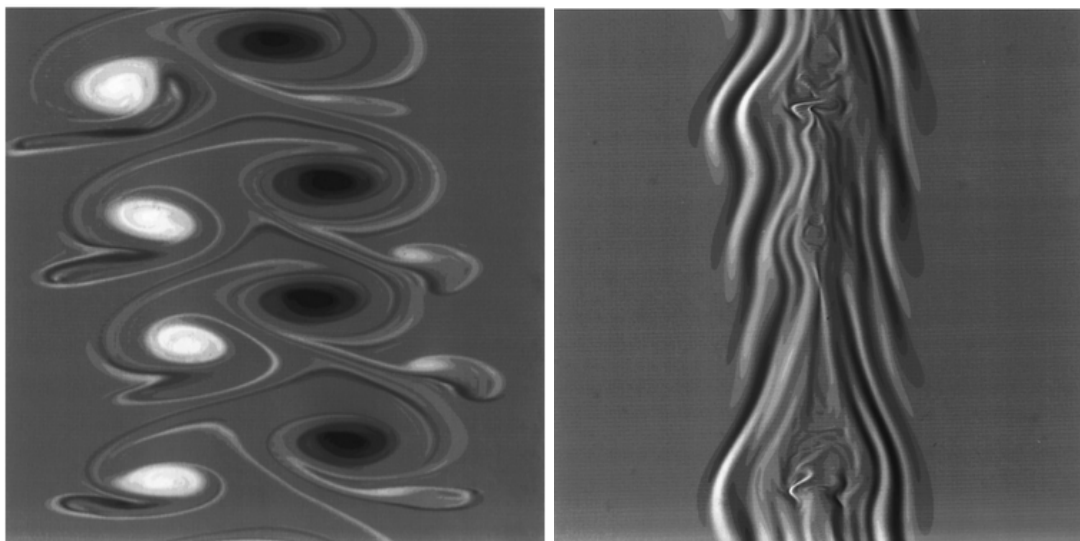


Figure 2. (a) Bickley Jet evolution of sinusoidal perturbation without magnetic field. [6]
 (b) Current Sheet evolution of sinusoidal perturbation with magnetic field. [6]

Since the current sheet has the Bickley Jet as the velocity profile, one might expect that the current sheet would also be unstable. However, the surrounding magnetic field acts as a guide for the jet and stabilizes the flow. This result was shown in a paper by Biskamp et al. [6]. The goal of this paper is to perform a systematic study on the evolution of the current sheet. I aim to find how a current sheet is affected by a perturbation in the velocity field and the effects of the resistivity and the magnetic field.

METHODS

I wrote a computer program in Python to simulate a current sheet with a perturbation. My code uses two differential equations to describe the system and compute the next time step. To solve the equations, I used the centered finite difference method to calculate derivatives. The simulation uses mixed boundary conditions: periodic for fluid flow and Neumann for the magnetic field. The aspect ratio of the system was 2:1; there were 128 grid points in the x direction and 64 in the y direction.

The equations governing the flow are written in terms of the vorticity ω (omega) and the magnetic flux function ψ (psi). Because the flow is incompressible, the fluid velocity is perpendicular to the gradient of the velocity potential ϕ (phi), which is obtained from the vorticity by solving the Poisson equation shown below. Likewise, the magnetic field is perpendicular to the gradient of the magnetic flux function ψ (psi). The governing equations are as follows [6]:

$$\partial_t \omega + \mathbf{v} \cdot \nabla \omega = \mathbf{B} \cdot \nabla j + \mu \nabla^2 \omega, \quad \text{Eq. (1)}$$

$$\partial_t \psi + \mathbf{v} \cdot \nabla \psi = \eta \nabla^2 \psi, \quad \text{Eq. (2)}$$

where the velocity, magnetic field, vorticity, and current density are defined by

$$\begin{aligned} \mathbf{v} &= \mathbf{e}_z \times \nabla \phi & \mathbf{B} &= \mathbf{e}_z \times \nabla \psi \\ \omega &= \nabla^2 \phi & j &= \nabla^2 \psi \end{aligned}$$

In these equations, μ (mu) is fluid viscosity and η (eta) is magnetic resistivity.

Computer codes need verification tests to make sure they are written correctly and produce sensible results. For this purpose, I wrote several versions of the code, adding capabilities for each update.

To speed up the code, I used GPU parallelization to compute the solution on GPU processors. I used the Python library CuPy to speed up the code by converting my Numpy arrays into CuPy arrays that are processed by the GPU.

In the following subsections, I will explain the verification and optimization methods I have used.

Verification

In Eqs. (1) and (2), the fluid motion is described by diffusion and advection. The diffusion term is the second derivative in space and advection is the first derivative in space, multiplied by velocity. I tested the diffusion and advection terms separately in 1D and 2D settings. Then I tested the full equations, having both diffusion and advection activated.

(1) In a very simple version of my code, I had a one-dimensional system described by Eq. (1) with only the diffusion term. The initial condition was a sine wave. The system has an analytical solution:

$$u_{ext} = A \sin(2\pi x/L) e^{-4\mu\pi^2 t/L^2}$$

Running my code, I expected to find an answer equal to the exact solution. There was some discrepancy due to numerical approximations in the calculations. I found that the root mean squared (RMS) difference between the numerical and exact solutions was of order 0.1%.

(2) I solved Eq. (1), again with just the diffusion term, in two dimensions. The initial conditions were, however, quasi-1D, meaning there was no variation in the y direction. For each value of y, the RMS difference between the numerical and exact solutions was of order 0.1%.

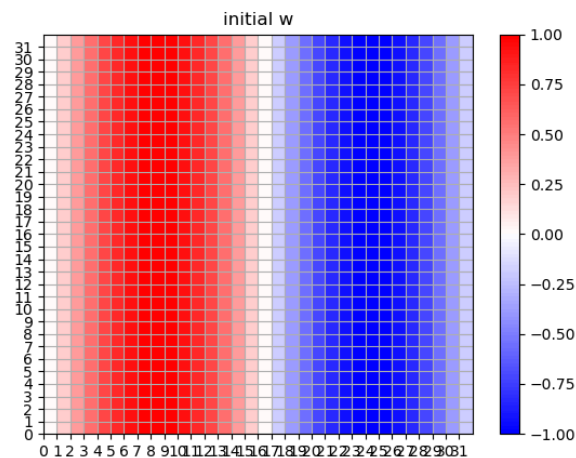


Figure 3. Initial vorticity profile for (2). X and y are spatial dimensions.

(3) The previous tests only involved the diffusion term. The next test used only the advection term. Equation (1) is used in two dimensions without the diffusion or magnetic term. In this test, to find the velocity, my code solves the Poisson equation for ϕ . The initial condition was a circular Gaussian bump in the vorticity, ω . Because the vorticity field was circular, the velocity is angular and the advection term should be zero. The RMS difference between the vorticity at the final and initial times was of order 0.0001%.

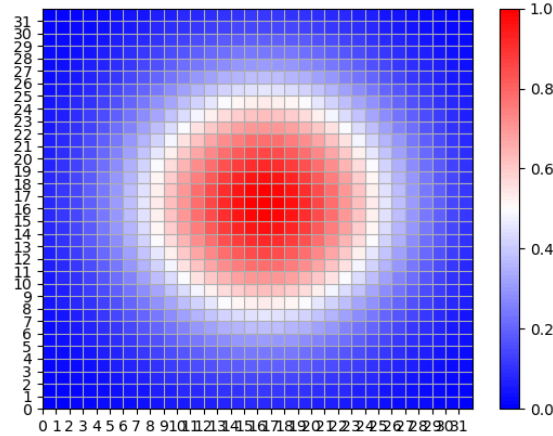


Figure 4. Initial vorticity profile for (3). X and y are spatial dimensions.

(4) I again tested the advection term in Eq. (1), but now with an added diagonal velocity. Because of the periodic boundary conditions, the bump should move diagonally, exit through the top right corner, enter through the bottom left corner, and return to the center. The RMS difference was again calculated between the final time step and the initial condition. The difference was of order 1%, which is relatively large. It could be reduced by using a better time-stepping method or by refining the grid. Nonetheless, the difference is small enough to show that my code is correctly solving the equations and the difference is due to numerical approximations.

(5) Next, I tested the advection term without an added velocity, meaning that the velocity field is induced by the vorticity. I tested my code with two vortices. The flow is too complex to have an analytic solution, so the simulation was verified only by observing its qualitative behavior. These initial conditions are well-known in fluid dynamics, so I knew that the two vortices should merge at the center after swirling around each other for a while.

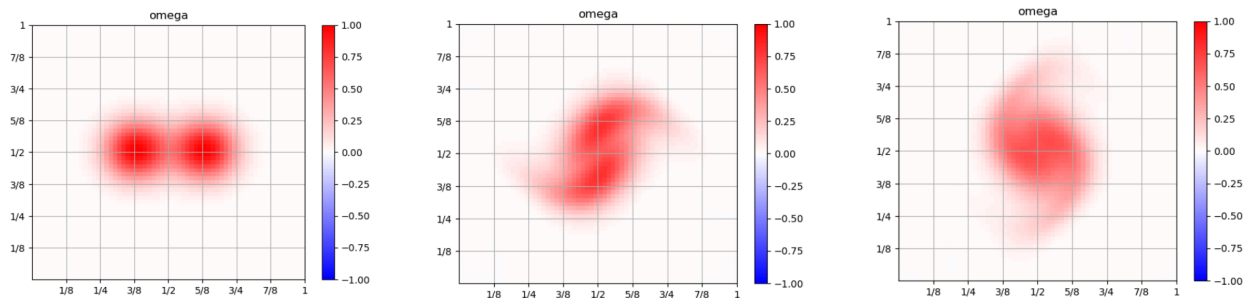


Figure 5. Plots of vorticity showing the evolution through time. X and y are spatial dimensions.

(6) I tested my code using the initial conditions of the Bickley Jet. This is the velocity profile of the current sheet, which is known to be a steady-state but unstable solution. Steady-state means that the system should not change in time. The RMS difference was calculated between the final time step and the initial condition. The error was of order 0.1%.

Procedure

The velocity and magnetic field profiles in a current sheet are modeled by:

$$v_y(x, y) = V_0 \operatorname{sech}^2(x),$$

$$B_y(x) = B_0 \tanh(x),$$

from which I calculate vorticity and the flux function as

$$\omega(x, y) = V_0 \frac{\tanh(x)}{\cosh(x)},$$

$$\psi(x) = B_0 \ln(\cosh(x)).$$

Then I apply a perturbation to the vorticity field to get the initial conditions for the simulations:

$$\omega(x, y) = V_0 \frac{\tanh(x)}{\cosh(x)} * \mathit{pert}$$

$$\text{with } \mathit{pert} = A \sin(ky)$$

I set the code to run 1,800 time steps and to plot intermittently.

Optimizations

My code, like other Direct Numerical Simulations (DNS), takes significant computational power and time. Since several runs are needed to get the results I present, optimization of my program is necessary. It drastically lowers the effort needed and quickens debugging, which takes the majority of development time. In my project, several strategies were followed to reduce the run time of my program. In the first full version of my code, the run time for a full simulation took almost 2 hours. Using the NumPy library, I vectorized my equations. When, for example, adding two arrays, vectorization makes the computer add every entry at once rather than one at a time. For my program, this reduced the run time to 1 ½ hours. Then, with a library called CuPy, I utilized the GPU to parallelize my program, which reduced the runtime to 1 hour. GPU parallelization involves spreading calculations among many GPU processors. Normally, the computer uses the CPU, which has only a few processors, each very powerful. In contrast, GPU processors are relatively weak, but there are thousands of them. For a DNS, the GPU is much more efficient. Finally, by using a sparse matrix solver in the SciPy library, I reduced the computational time to 8 minutes. To solve the Poisson equation that describes the relationship between ϕ (phi) and ω (omega), $\omega = \nabla^2 \phi$, I represented the Laplacian operator (∇^2) as a sparse matrix and used a sparse matrix solver. After this conversion, the runtime was drastically reduced.

RESULTS

The equations in my code use vorticity to describe the flow of the plasma instead of velocity; this approach simplifies the calculations. Vorticity is a measure of swirling motion, like in a hurricane. A hurricane is a vortex in which the wind swirls around the center in a circular motion. A positive value of vorticity indicates a vortex that is spinning counter-clockwise, whereas a negative value corresponds to a clockwise spin.

The first series of plots (Figure 6) shows the vorticity profile of the perturbed current sheet without a magnetic field. The second series of plots (Figure 7) has a magnetic field with an amplitude of 0.3, which leads to different results for the same initial vorticity profile.

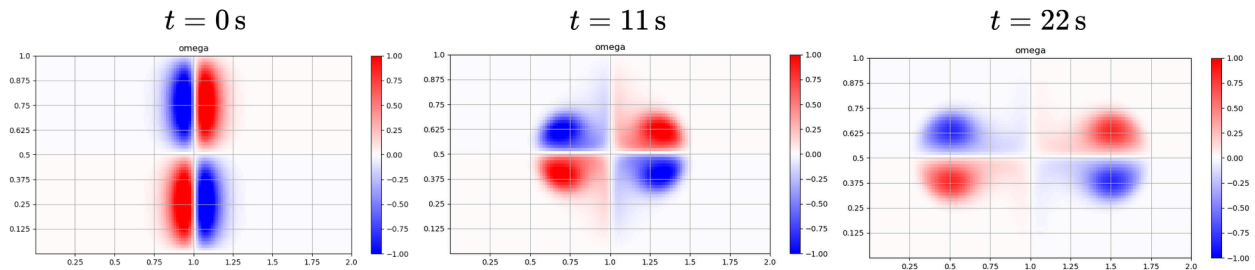


Figure 6. Evolution of vorticity in the non-magnetized current sheet. X and y are spatial dimensions

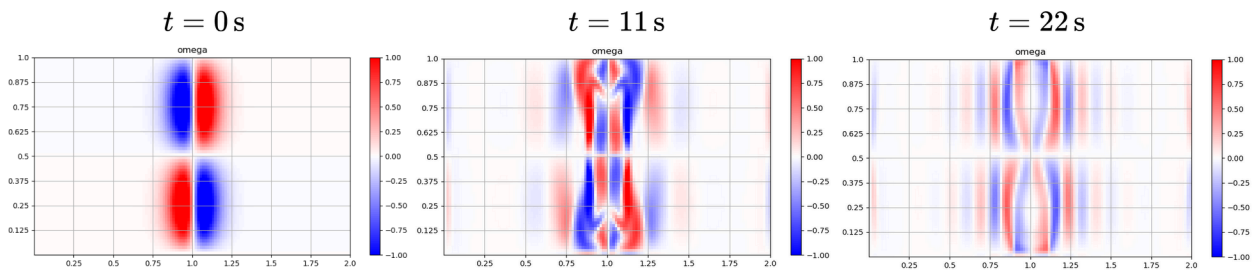


Figure 7. Evolution of vorticity in the magnetized current sheet. X and y are spatial dimensions

Furthermore, I ran a parameter study of the current sheet by varying the resistivity and the magnetic field strength (Figure 8). Each plot in Figure 8 shows the vorticity profile of the current sheet after 22.5 seconds.

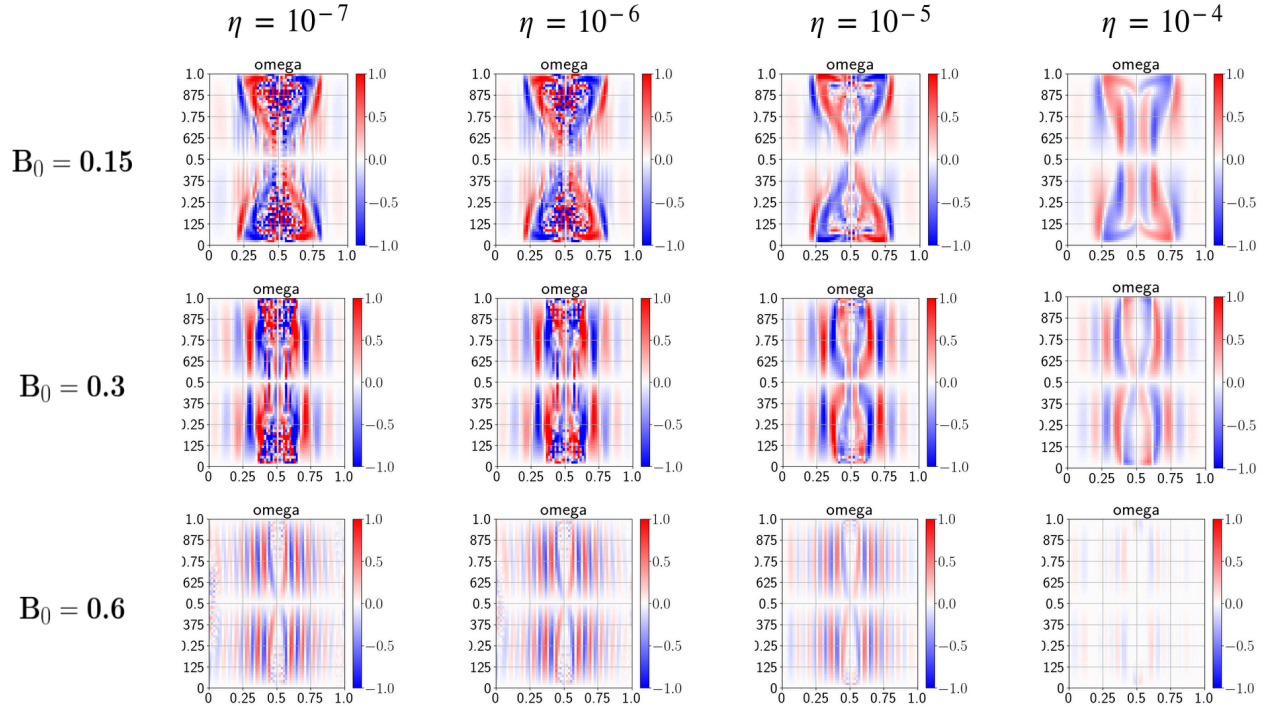


Figure 8. The final vorticity profile with different values of resistivity and magnetic field strength. X and y are spatial dimensions.

I then calculated the L2 norm of the vorticity profiles to make a quantitative measure of stability:

$$\|\omega\|_2 = \sqrt{\frac{\sum_{i,j} (\omega_{i,j})^2}{N}}$$

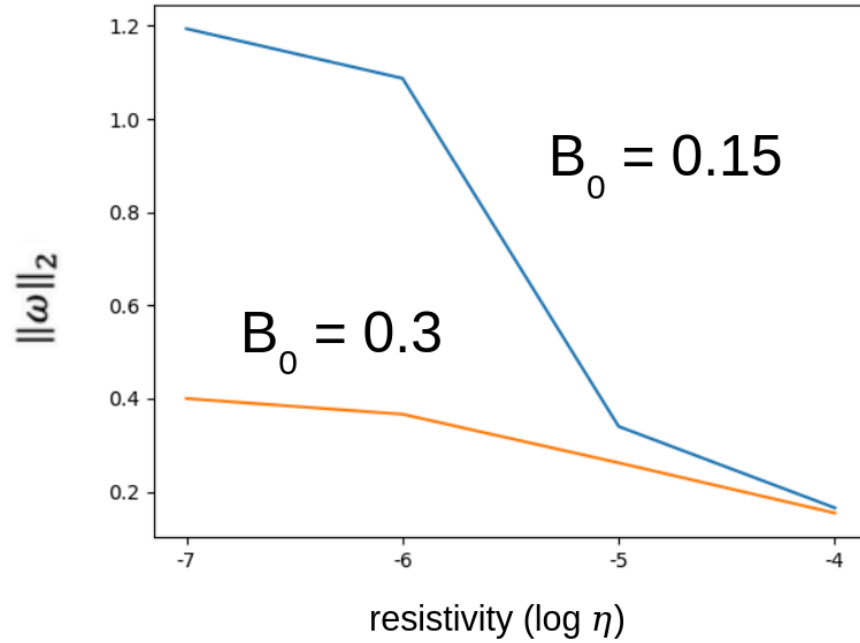


Figure 9. L2 norm of the vorticity profiles. The blue line is for $B_0 = 0.15$ and the orange line is for $B_0 = 0.3$. For a fixed magnetic field strength, an increase in resistivity leads to a lower L2 norm of vorticity. This implies that the flow is more stable.

Here I show the average magnetic energy at the final timestep for different initial conditions:

$$e_B = \frac{B^2}{2\mu_0}$$

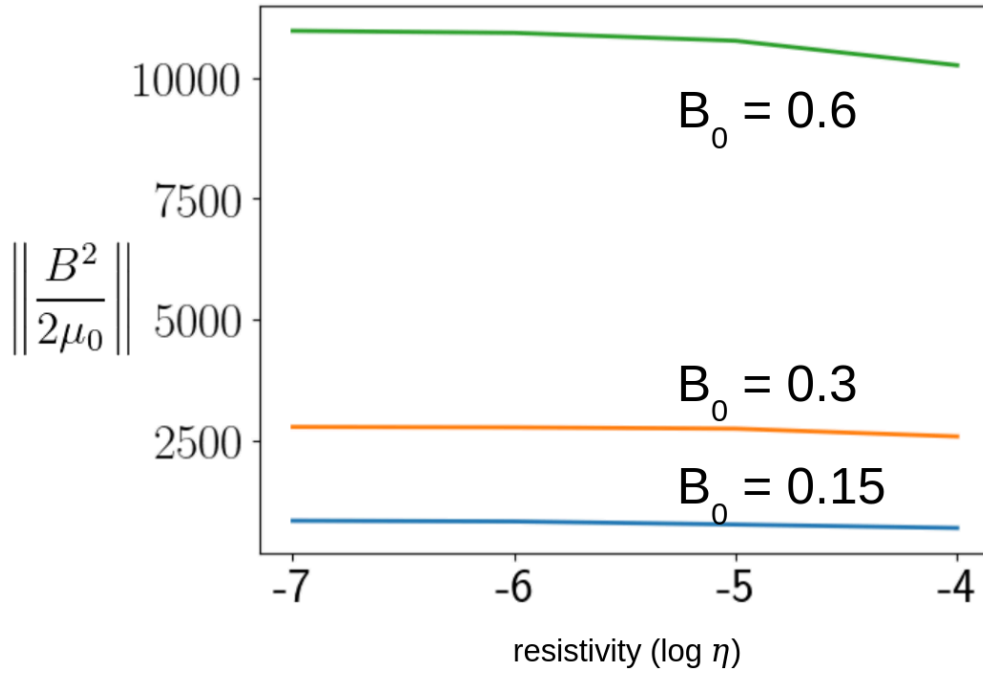


Figure 10. Average magnetic energy. The blue line is for $B_0 = 0.15$, the orange line is for $B_0 = 0.3$, and the green line is for $B_0 = 0.6$.

CONCLUSIONS

In the first series of plots (Figure 6), pairs of vortices push out to the sides due to the perturbation; this shows that the system is unstable to the perturbation. The cause is that the pairs of vortices induce advection. Like a hand mixer, a pair of opposite sign vortices push fluid behind them, so that they are pushed forward. This leads the two pairs of vortices to collide in the center and then spread outwards.

In the second series (Figure 7), the results are strikingly different. The jet merely broadens, showing the same qualitative behavior as in the paper by Biskamp et al. [6]. The magnetic field stabilizes the flow.

After confirming that the magnetic field stabilizes the current sheet, I further tested the current sheet by varying the strength of the magnetic field and the plasma resistivity. As mentioned earlier, each plot in Figure 8 is the vorticity profile of the current sheet at 22.5 seconds. As can be seen in the plots, increasing the resistivity (η) has a stabilizing effect. As well as the resistivity, the magnetic field strength also has a huge effect. Also, note that the difference between the profiles for $B_0 = 0.6$ is very small despite the changes in resistivity.

This is further demonstrated by the L2 norm graph (Figure 9). As the resistivity is increased, the L2 Norm goes down, meaning a less turbulent vorticity profile. The orange line, for $B_0=0.3$, has less turbulence than the blue line, for $B_0=0.15$, again showing that the magnetic field stabilizes the current sheet.

From Figure (10) we find that magnetic energy is mainly determined by the initial magnetic field strength and is relatively insensitive to the resistivity.

These results show that current sheets with strong enough magnetic fields and high enough resistivity are stable to perturbation while maintaining high magnetic energy. In the case of coronal arches, both are strong enough to make the current sheet stable. If the current sheets were unstable, magnetic reconnection would not occur according to the Sweet-Parker model. The stability of the current sheet facilitates magnetic reconnection to occur. My project shows that the Sweet-Parker model can describe magnetic reconnection for when coronal arches form solar flares and Coronal Mass Ejections.

BIBLIOGRAPHY

[1] Solar storms could cost USA tens of billions of dollars. University of Cambridge. (2017, January 19). <https://www.cam.ac.uk/research/news/solar-storms-could-cost-usa-tens-of-billions-of-dollars>

[2] May, A., & Dobrijevic, D. (2022, May 20). *The carrington event: History's greatest solar storm*. Space.com. <https://www.space.com/the-carrington-event>

[3] Laboratory, L. A. N. (n.d.). Forecasting space weather: Discover los alamos national laboratory. LANL Discover RSS. <https://discover.lanl.gov/publications/national-security-science/2022-spring/vania-jordanova/>

[4] Coronal mass ejections. Coronal Mass Ejections | NOAA / NWS Space Weather Prediction Center. (n.d.). <https://www.swpc.noaa.gov/phenomena/coronal-mass-ejections>

[5] Gurnett, D. A., & Bhattacharjee, A. (2017). *Introduction to plasma physics: With space, laboratory and Astrophysical Applications*. Cambridge University Press.

[6] Biskamp, D., Schwarz, E., & Zeiler, A. (1998). Instability of a magnetized plasma jet. *Physics of Plasmas*, 5(7), 2485–2488. <https://doi.org/10.1063/1.872931>

ACKNOWLEDGEMENTS

I want to thank my mentors for their support in my project and in writing this paper.

Mark Petersen guided me through writing my code and provided helpful insights.

JeeYeon Plohr helped with the research and execution of my project as well as the presentation.

Bradley Plohr helped me conceptualize much of the mathematics required.